CrystEngComm

PAPER

View Article Online
View Journal | View Issue

Cite this: *CrystEngComm*, 2014, **16**, 7673

Solvent-mediated assembly of chiral/achiral hydrophilic Ca(II)-tetrafluoroterephthalate coordination frameworks: 3D chiral water aggregation, structural transformation and selective CO_2 adsorption†

Sheng-Chun Chen,[ab] Feng Tian,[a] Kun-Lin Huang,*[c] Cheng-Peng Li,[d] Jing Zhong,[a] Ming-Yang He,[ab] Zhi-Hui Zhang,[a] Hong-Ning Wang,[a] Miao Du*[d] and Qun Chen*[ab]

Received 21st May 2014,
Accepted 26th June 2014

DOI: 10.1039/c4ce01019a

www.rsc.org/crystengcomm

The spontaneous self-assembly reactions of 2,3,5,6-tetrafluorobenzenedicarboxylic acid ($H_2BDC\text{-}F_4$) with $Ca(NO_3)_2{\cdot}4H_2O$ in different solvents resulted in the generation of hydrophilic 3D chiral and achiral Ca(II)–organic frameworks $\{[Ca_4(BDC\text{-}F_4)_4(H_2O)_4]{\cdot}4H_2O\}_n$ (**1**) and $[Ca(BDC\text{-}F_4)(MeOH)_2]_n$ (**2**), respectively. Complex **1** exhibits higher water solubility compared to **2**, and further dissolution of **1** in water results in a new achiral crystal, $[Ca(BDC\text{-}F_4)(H_2O)_4]_n$ (**3**). All complexes have been characterized by elemental analysis, IR spectroscopy, and single-crystal and powder X-ray diffraction techniques. Complex **1** crystallizes in the tetragonal $P4_12_12$ chiral space group and features a rare binodal 5-connected network, directed by a unique 3D chiral (10,3)-*a* water aggregation consisting of two distinct helical arrays. Complex **2** crystallizes in the space group *C*2/*c* and has a binodal 4-connected **pts** net. Complex **3** crystallizes in the space group $P2_1/m$ and presents a 2D layer framework containing the unprecedented polymeric $[Ca^{II}\text{–}H_2O]_n$ chain based on triple μ_2-O aqua bridges. The structural discrepancies illustrate the solvent-induced effect on the construction and structural transformation of chiral and achiral coordination frameworks. Moreover, gas (N_2 and CO_2) adsorption studies show that the dehydrated framework **1a** exhibits excellent selective CO_2 gas uptake at 195 K.

Introduction

Metal–organic frameworks (MOFs) have been considered as a promising class of porous crystalline materials with potential applications in gas sorption/separation, catalysis, magnetism, and photoluminescence.[1] The main advantage of MOFs over traditional porous materials is their highly designable nature, which allows the pore size, shape and even the inner surface to be adjusted. The versatile pore features of MOFs, such as Lewis acidity, basicity, hydrophilicity, and chirality, can be modified by varying the combination of organic ligands and metal ions.[2] Thus, porous MOFs bearing different functional groups in the channels or voids have also been envisioned as ideal hosts for capturing various guests and also affecting their distributions, which may lead to a precise control of the stereoregularity of the resulting lattices. In this connection, MOFs with helical or chiral functionalities on the pore surfaces are of special interest.[3] For instance, Banerjee *et al.* have recently constructed a series of chiral MOFs with halogen-substituting ligands and continuous helical water chains within the pores.[4] However, investigation on the chiral induction effect of guest species on MOFs is still a great challenge.

Thus far, a variety of structurally definite water aggregates, such as discrete water clusters,[5] and infinite 1D chains,[6] 2D layers,[7] or 3D water networks[8] have been observed in diverse crystalline hosts. Very recently, Wu *et al.* have reported the first example of chiral metallocycle templating of a 3D chiral zeolite-like water network comprising uniform *P* helical water chains.[9] Indeed, helical water motifs are broadly attractive due to their fundamental importance in biological processes related to water and ion transport.[10] A practical approach to organize helical water chains is to employ chiral organic

[a] *School of Petrochemical Engineering, Jiangsu Key Laboratory of Advanced Catalytic Materials and Technology, Changzhou University, Changzhou 213164, PR China. E-mail: chenqunjpu@yahoo.com*
[b] *School of Chemical Engineering, Nanjing University of Science & Technology, Nanjing 210094, PR China*
[c] *College of Chemistry, Chongqing Normal University, Chongqing 401331, PR China*
[d] *College of Chemistry, Tianjin Key Laboratory of Structure and Performance for Functional Molecules, MOE Key Laboratory of Inorganic-Organic Hybrid Functional Material Chemistry, Tianjin Normal University, Tianjin 300387, PR China. E-mail: dumiao@public.tpt.tj.cn*

† Electronic supplementary information (ESI) available: Selected bond lengths and angles, TGA curves of 1–3, powder X-ray diffraction patterns, and crystallographic data (in CIF format). CCDC 1003028–1003030. See DOI: 10.1039/c4ce01019a

synthons or achiral multifunctional ligands with rich H-bonding groups.[11] In this respect, halogenated compounds are of particular interest as the noncovalent hydrogen and halogen bonds may improve the probability of creating supramolecular water helices.[4,12]

In our efforts to explore perfluorinated MOF materials,[13] we have illustrated the fluorine-induced coordination assembly of chiral networks by a flexible achiral Schiff base, where helical water chains play a key role.[13b] In this contribution, we initiate the realization of chiral discrepancy with solvent-regulation assembly of two 3D Ca^{II} MOFs: chiral $\{[Ca_4(BDC\text{-}F_4)_4(H_2O)_4]\cdot 4H_2O\}_n$ (**1**) and achiral $[Ca(BDC\text{-}F_4)(MeOH)_2]_n$ (**2**) constructed from rigid achiral tetrafluoroterephthalic acid ($H_2BDC\text{-}F_4$) in different solvent media. Remarkably, the unusual 5-connected coordination framework of **1** encapsulates a unique 3D chiral water network constructed from two distinct helical arrays, while **2** displays a binodal 4-connected **pts** network. Moreover, compared to **2**, **1** is highly water-soluble, and further evaporation of **1** in water results in an achiral 2D MOF, $[Ca(BDC\text{-}F_4)(H_2O)_4]_n$ (**3**), revealing the water-induced structural transformation from chirality to achirality. In addition, the dehydrated framework **1a** exhibits a high gas adsorption selectivity to CO_2 over N_2 at 195 K.

Experimental

Materials and general methods

All reagents and solvents for synthesis and analysis were commercially available and used as received. The Fourier transform (FT) IR spectra (KBr pellets) were recorded on a Nicolet ESP 460 FT-IR spectrometer. Elemental analyses of carbon, hydrogen and nitrogen were performed on a PE-2400II (Perkin-Elmer) analyzer. Powder X-ray diffraction (PXRD) patterns were recorded on a Rigaku D/Max-2500 diffractometer at 40 kV and 100 mA with a Cu-target tube (λ = 1.5406 Å). The calculated PXRD patterns were obtained from the single-crystal diffraction data using the PLATON software.[14] Thermogravimetric analysis (TGA) experiments were carried out using a DuPont thermal analyzer from room temperature to 800 °C at a heating rate of 10 °C min^{-1} under nitrogen stream. The molar electrical conductivity was measured in 10^{-3} M aqueous solution at 25 °C with a Radelkis OK 102/1 conductometer.

Syntheses of complexes 1–3

$\{[Ca_4(BDC\text{-}F_4)_4(H_2O)_4]\cdot 4H_2O\}_n$ (1). An ethanol solution (6 mL) of $H_2BDC\text{-}F_4$ (71.4 mg, 0.3 mmol) was added to a DMF–ethanol solution (12 mL/6 mL) of $Ca(NO_3)_2\cdot 4H_2O$ (70.8 mg, 0.3 mmol) in a beaker. After *ca.* 30 min of stirring, the colorless solution was filtered and left to stand at room temperature. After seven weeks, colorless needle-like crystals of **1** suitable for X-ray diffraction were obtained by slow evaporation of the solvents in 62% yield (58.1 mg, based on $H_2BDC\text{-}F_4$). Anal. calcd. for $C_8H_4CaF_4O_6$ (**1**): C, 30.78; H, 1.29%. Found: C, 30.49; H, 1.63%. IR (cm^{-1}): 3565 s, 3509 bs, 1671 s, 1601 s, 1495 m, 1466 s, 1390 vs, 1283 m, 1262 m, 1105 m, 1032 w, 990 s, 908 w, 821 w, 781 m, 669 m, 623 m.

$[Ca(BDC\text{-}F_4)(MeOH)_2]_n$ (2). The same synthetic procedure as that for **1** was used except that the ethanol solvent was replaced with methanol (6 mL), affording colorless block crystals of **2** in 52% yield (53.1 mg, based on $H_2BDC\text{-}F_4$). Anal. calcd for $C_{10}H_8CaF_4O_6$ (**2**): C, 35.30; H, 2.37%. Found: C, 34.92; H, 2.41%. IR (cm^{-1}): 3457 bs, 2967 m, 2885 m, 1653 s, 1611 s, 1490 m, 1465 s, 1392 s, 1262 m, 1253 m, 1112 m, 1063 w, 986 s, 886 m, 799 m, 756 s, 673 m, 663 w.

$[Ca(BDC\text{-}F_4)(H_2O)_4]_n$ (3). Complex **1** (1249.0 mg, 4 mmol) was dissolved in pure water (12 mL). Upon slow evaporation of the solution over five weeks, colorless needle-like crystals of **2** were obtained in 76% yield (949.0 mg, based on **1**). Anal. calcd. for $C_8H_8CaF_4O_8$ (**2**): C, 27.59; H, 2.32%. Found: C, 27.83; H, 2.68%. IR (cm^{-1}): 3565 s, 3504 bs, 1647 s, 1613 s, 1498 m, 1465 s, 1390 vs, 1261 m, 990 s, 908 w, 782 m, 690 m, 625 m.

Sorption measurements

The gas sorption isotherms were measured using an ASAP 2020M adsorption instrument. The as-synthesized material was treated by heating at 160 °C for 6 h in a quartz tube under vacuum to remove the solvent molecules prior to measurement.

X-ray crystallography

Single-crystal X-ray diffraction measurements of **1–3** were performed on a Bruker APEX II CCD diffractometer at ambient temperature with Mo Kα radiation (λ = 0.71073 Å). For each measurement, a semiempirical absorption correction was applied using SADABS, and the program SAINT was used for integration of the diffraction profiles.[15] The structures were solved by direct methods and refined by full-matrix least-squares on F^2 using the SHELXTL program.[16] All non-hydrogen atoms were refined anisotropically. C-bonded hydrogen atoms were placed in geometrically calculated positions by using a riding model. O-bound hydrogen atoms were localized in difference Fourier maps and refined in subsequent refinement cycles. The details of crystallographic parameters, data collection and refinements for the complexes are listed in Table 1, and selected bond lengths and angles with their estimated standard deviations are listed in Table S1 (ESI†).

Results and discussion

Crystal structures of complexes 1–3

$\{[Ca_4(BDC\text{-}F_4)_4(H_2O)_4]\cdot 4H_2O\}_n$ (1). Single-crystal X-ray diffraction analysis reveals that complex **1** crystallizes in the chiral space group $P4_12_12$ with the absolute structure parameter (Flack parameter) of +0.05(1), indicating that each individual crystal consists of a single enantiomer.[17] The asymmetric unit of **1** consists of one Ca^{II} center, one $BDC\text{-}F_4$ dianion, one aqua ligand, and two half-occupied independent lattice water molecules. Each Ca^{II} ion is seven-coordinated in a distorted pentagonal bipyramidal geometry (CaO_7), defined by six carboxylate oxygen donors from five different $BDC\text{-}F_4$ dianions with Ca–O distances in the range of 2.335(3)–2.556(3) Å

Table 1 Crystallography data and details of diffraction experiments for complexes **1–3**

	1	2	3
Formula	$C_{32}H_{16}Ca_4F_{16}O_{24}$	$C_{10}H_8CaF_4O_6$	$C_8H_8CaF_4O_8$
M_r	1249.77	340.24	348.22
Crystal system	Tetragonal	Monoclinic	Monoclinic
Space group	$P4_12_12$	$C2/c$	$P2_1/m$
a/Å	14.835(1)	10.950(1)	3.739(1)
b/Å	14.835(1)	17.701(1)	22.568(7)
c/Å	6.785(1)	7.843(1)	6.767(2)
α/°	90	90	90
β/°	90	102.330(1)	93.286(6)
γ/°	90	90	90
V/Å^3	1493.4(2)	1485.0(1)	1049.3(4)
Z	1	4	2
D_c/g cm^{-3}	1.388	1.522	2.028
μ/mm^{-1}	0.478	0.488	0.650
R_{int}	0.0113	0.0358	0.0240
R,[a] R_w[b]	0.0525, 0.1287	0.0639, 0.2168	0.0298, 0.0791
GOF on F^2	1.042	1.035	1.067
Flack factor	0.05(1)	—	—

[a] $R = \sum||F_o| - |F_c||/\sum|F_o|$. [b] $R_w = \sum[w(F_o^2 - F_c^2)^2]/\sum[w(F_o^2)^2]^{1/2}$.

and one oxygen atom from one aqua ligand with a Ca–O distance of 2.270(1) Å (Fig. 1a). The BDC-F_4 ligand exhibits two different types of coordination modes with one carboxylate group displaying a μ_2-η^1:η^1-*syn–syn*-bridging mode and the other one displaying a μ_3-η^2:η^2-chelating/bridging mode to connect five Ca^{II} ions. Thus, the CaO_7 pentagonal bipyramids share edges and form 1D Ca–O–C rods running along the *c* axis (Fig. 1b). Moreover, each rod cross-links four neighboring rods through the perfluorinated benzene rings of BDC-F_4 ligands, generating a 3D rod-packing framework having square-shaped channels with a cross-section of *ca.* 14.8 × 14.8 Å^2 along the *c* axis, as indicated in Fig. 1c. Topological analysis revealed that compound **1** can be described as an **sra** net, as defined by the Reticular Chemistry Structure Resource,[18] or a rare binodal 5-connected network (Fig. 1d) with the Schläfli symbol of $\{4^3{\cdot}6^5{\cdot}8^2\}\{4^6{\cdot}6^4\}$, determined using TOPOS.[19] The channel interior is decorated with fluorine groups of BDC-F_4 ligands, making the fluorous pore surface highly polar. Calculation using PLATON[14] suggests that after the removal of all water molecules, the fluorine-lined channels possess a void volume of 1980.9 Å^3 (about 40.0% of the unit cell volume), which is comparable to that of **FMOF-1**.[20]

Remarkably, the lattice water molecules are included in the fluorine-lined channels, forming a chiral 3D water network *via* hydrogen bonding with the coexistence of two asymmetric helical arrays of water chains. The water molecules O2W and O3W and their symmetric ones are highly ordered to afford a water channel with *M*-helices along [001] (Fig. 2a), with a helical pitch the length of the *c* axis and the period of each repeating unit the length of the *b* axis. The average O···O distance in such a water helix is 2.592(1) Å, clearly shorter than the sum of their van der Waals radii (r_{vdW} for O = 1.52 Å), revealing the presence of strong noncovalent O···O interactions. Moreover, the O3W water molecules are hydrogen-bonded to each other (O···O3 = 2.934 Å), affording

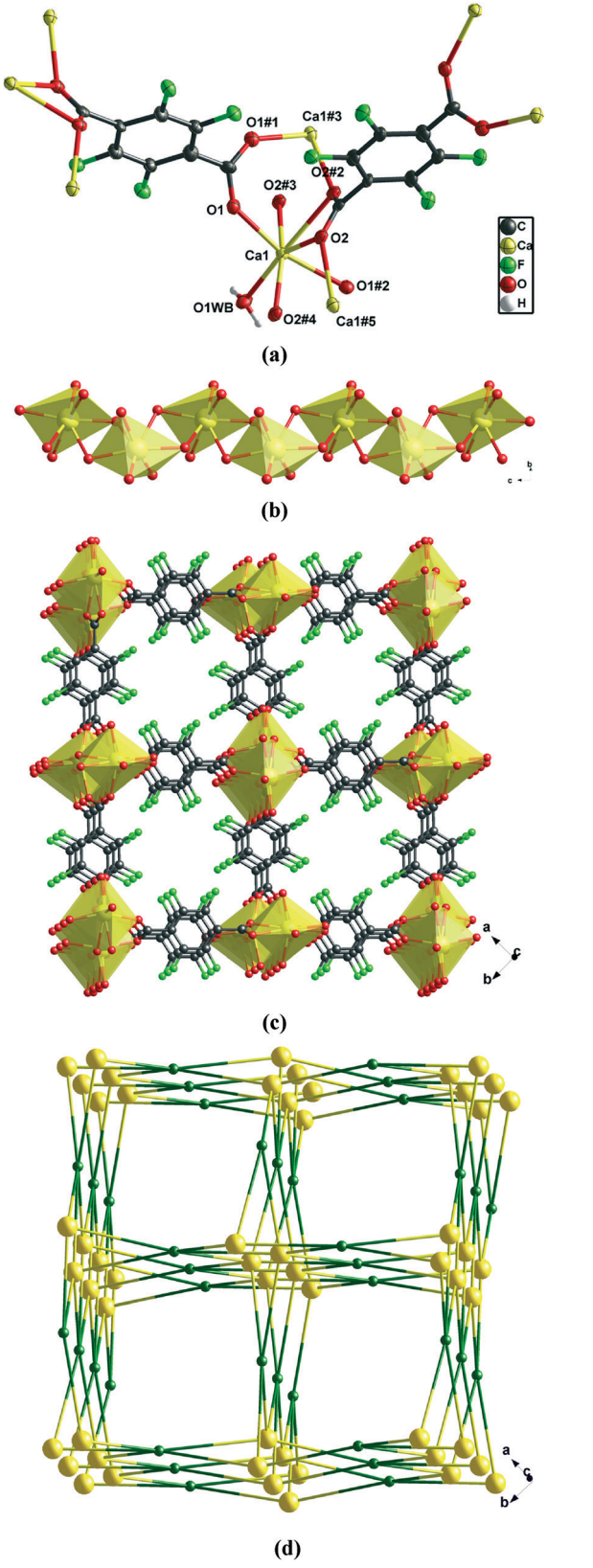

Fig. 1 Views of **1**: (a) the coordination environment of Ca^{II} and the binding mode of BDC-F_4. Symmetry codes: (1) −*x* + 1, −*y* + 1, −*z* + 5/2; (2) *x*, *y*, −*z* + 2; (3) −*x* + 1, −*y* + 1, *z* + 1/2; (4) −*x* + 1, −*y* + 1, −*z* + 3/2; (5) −*x* + 1, −*y* + 1, *z* − 1/2. (b) Polyhedral representation of the infinite 1D rod SBUs. (c) The 3D coordination framework. (d) A schematic representation of the 3D 5-connected network.

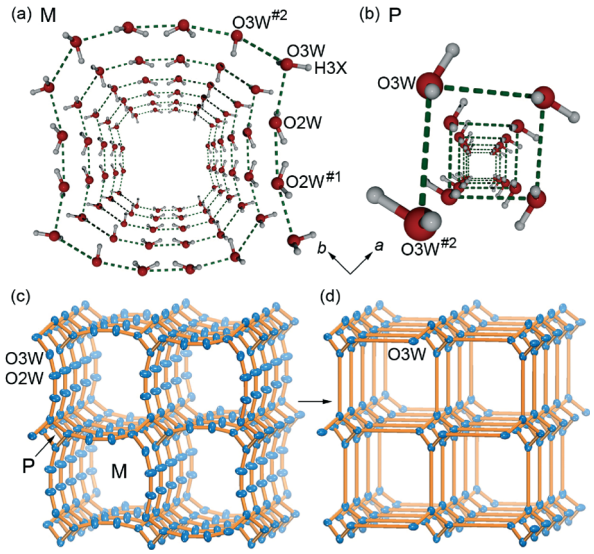

Fig. 2 (a) The 1D *M* helical water chain (O2W···O2W#1 = 2.451 Å; O2W···O3W = 2.521 Å; O3W···O3W#2 = 2.934 Å, symmetry codes: #1 = *x*, *y*, −*z*; #2 = −*x* + 1/2, *y* + 1/2, *z* − 1/4); (b) the 1D *P* helical water chain (O3W···O3W#2 = 2.934 Å, symmetry code: #2 = −*x* + 1/2, *y* + 1/2, *z* − 1/4); (c) the 3D chiral water net constructed by asymmetric *P* and *M* helical water motifs; (d) the simplified 3D H-bonding water network with (10,3)-*a* topology.

a smaller channel with *P*-helical (right-handed) C4 water chains along the *c* axis (Fig. 2b).[21] Notably, the O3W–O3W$^{\#2}$–O3W angle (109.5°) agrees well with the preferred tetrahedral arrangement for ice I_h,[22] which further indicates the similarity between helical C4 water morphology and ice I_h. These two types of helical water motifs are further combined through O3W molecules to afford a 3D H-bonding network with (10,3)-*a* topology (Fig. 2c and d). To the best of our knowledge, although symmetric helical water chains have been known,[23] such helical motifs in **1** containing simultaneously asymmetric *M* and *P* helical water in the same lattice have not been observed so far. In addition, weak O2W–H2X···F1 (O···F: 2.877 Å, angle: 146.4°) and O3W–H3X···F1 (O···F: 2.940 Å, angle: 119.2°) bonds between the fluorinated host framework and the encapsulated water aggregate are found. Thus, the fluorine groups of the coordination framework host can be considered as the structure-directing agent to determine the orientations of the helical water arrays and in turn transfer the chirality. The helical water morphologies act as a "guest helix" to be fixed within the perfluorinated host framework.

[Ca(BDC-F$_4$)(MeOH)$_2$]$_n$ (2). Complex **2** crystallizes in the centrosymmetric space group *C*2/*c* and contains one Ca^{II} centre, one deprotonated BDC-F$_4$ and two coordinated methanol ligands. The Ca^{II} ion is octahedrally coordinated (CaO$_6$) to four different BDC-F$_4$ ligands with Ca–O distances of 2.339(4) and 2.457(4) Å and to two terminal methanol ligands with a Ca–O distance of 2.377(4) Å (Fig. 3a). The BDC-F$_4$ ligand is linked to four Ca^{II} ions with each carboxylate group adopting the μ_2-η^1:η^1-*syn–anti*-bridging mode. The CaO$_6$ octahedra are repeated infinitely in the *c* axis, generating a linear Ca–O–C rod (Fig. 3b), which is linked to four neighboring rods by the tetrafluorinated benzene rings of BDC-F$_4$, resulting in the 3D framework (Fig. 3c) with the **sra** net topology that is similar to that of **1**. However, from a topological perspective, if each Ca^{II} ion is regarded as a four-connected tetrahedral node and each BDC-F$_4$ as a square building block, the resulting 3D structure of **2** can be described as a binodal 4-connected **pts** net with the Schläfli symbol of $\{4^2{\cdot}8^4\}$ (Fig. 3d). In addition, owing to

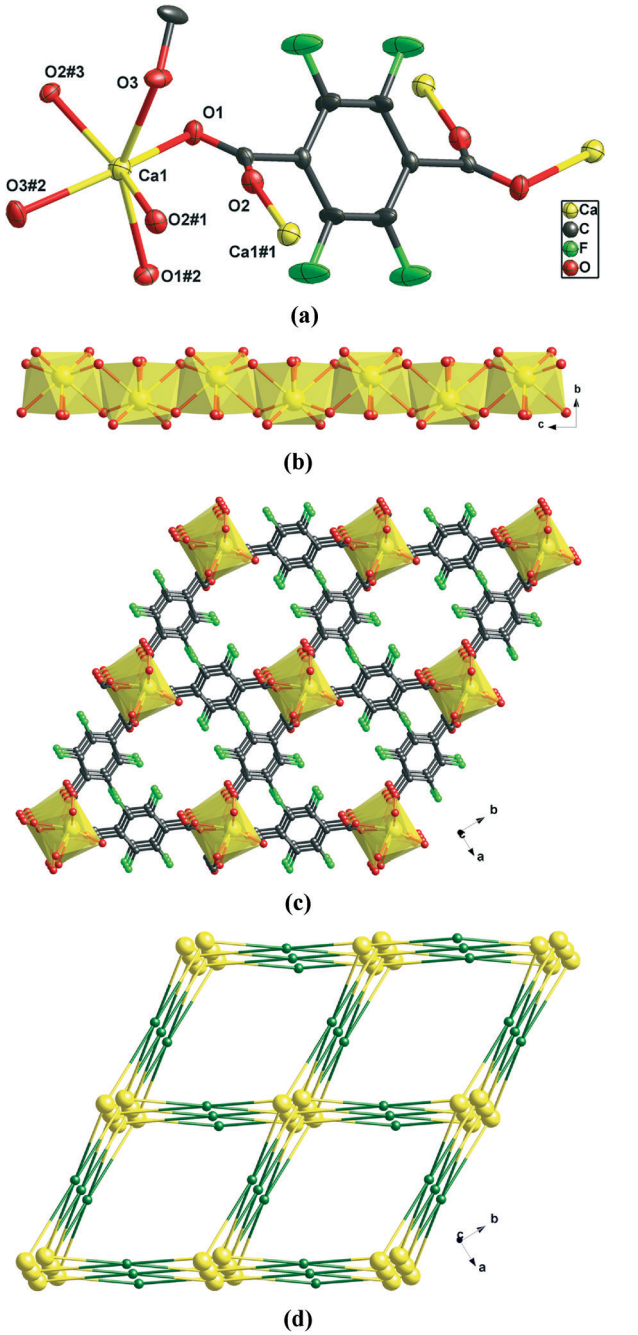

Fig. 3 Views of **2**: (a) the coordination environment of Ca^{II} and the binding mode of BDC-F$_4$. Symmetry codes: (1) −*x* + 1, −*y* + 1, −*z*; (2) −*x* + 1, *y*, −*z* + 1/2; (3) *x*, −*y* + 1, *z* + 1/2. (b) Polyhedral representation of the infinite 1D rod SBUs. (c) The 3D coordination framework. (d) A schematic representation of the 3D 4-connected network with **pts** topology.

the existence of obstructive terminal methanol entities that point toward the rhombus-shaped channels, such a 3D framework has very small voids of 84.2 Å^3 (only 5.7% of the unit cell volume) as calculated by PLATON.[14]

[Ca(BDC-F_4)(H_2O)$_4$]$_n$ (3). X-ray structural analysis reveals that **3** crystallizes in the space group $P2_1/m$ and shows a 2D layer framework, different from the 3D chiral structure of **1**. The asymmetric unit of **3** is composed of one Ca^{II} ion, one BDC-F_4 dianion and four aqua ligands. As shown in Fig. 4a, each Ca^{II} center is nine-coordinated by two BDC-F_4 ligands and seven water molecules with Ca–O distances in the range of 2.428(3)–2.598(2) Å. In **3**, the centrosymmetric BDC-F_4 ligand adopts the monodentate coordination mode for each carboxylate to bridge two Ca^{II} ions. Two adjacent Ca^{II} ions are linked by three μ_2-O atoms of aqua ligands to construct a 1D [Ca–H_2O]$_n$ chain (Fig. 4b). It should be emphasized that polymeric chains of aqua–metal complexes of s-block metals are quite limited. In fact, only several complexes consisting of 1D aqua–metal chains have been reported[24] where the adjacent metal centers are bridged by two water molecules. Further, infinite aqua–metal species with triple μ_2-O aqua bridges are even rare and only found for metal ions such as Na^{I},[25] K^{I},[26] and Sr^{II}.[27] To our knowledge, complex **3** represents the first example of a [Ca–H_2O]$_n$ chain based on triple aqua bridges.

Such 1D [Ca–H_2O]$_n$ motifs are extended by BDC-F_4 spacers to afford a 2D wave-like layer (Fig. 4c), where the adjacent Ca···Ca distances separated by BDC-F_4 and H_2O ligands are 12.563(3) and 3.739(1) Å, respectively. Further investigation of the crystal packing of **3** suggests that the adjacent layers are stacked parallel to the [001] direction and are interconnected *via* interlayer O–H···O H-bonding interactions between the coordinated water molecules and the uncoordinated carboxylate oxygen atoms of BDC-F_4 to realize the final 3D supramolecular architecture.

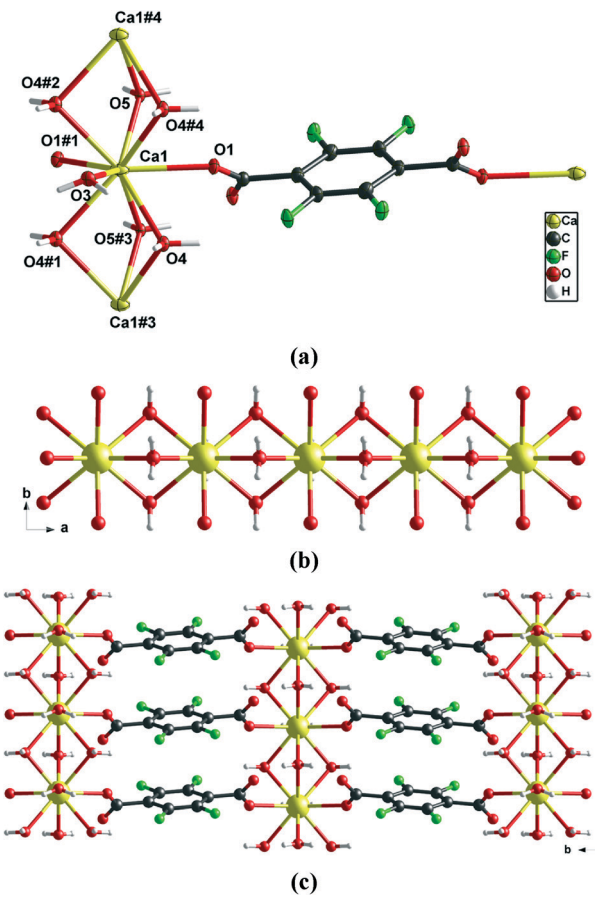

Fig. 4 Views of **3**: (a) the coordination environment of Ca^{II} and the binding mode of BDC-F_4. Symmetry codes: (1) x, $-y + 3/2$, z; (2) $x + 1$, $-y + 3/2$, z; (3) $x - 1$, y, z; (4) $x + 1$, y, z. (b) The 1D [Ca–H_2O]$_n$ chain based on triple aqua bridges. (c) The 2D layered structure along the *ab* plane.

Solvent effect and water-induced structural transformation

It was realized that solvents play an important role in the design and synthesis of coordination networks and supramolecular assemblies. Solvents with different sizes and coordination abilities not only facilitate the crystallization of well-defined molecular architectures but also trigger physicochemical properties such as adsorption, magnetism, catalysis, chirality, *etc.*[28] In particular, the solvent-dependent structural assemblies of chiral coordination compounds based on achiral ligands have been recently reported, although they are very rare.[29] Complexes **1** and **2** were synthesized in different solvent systems (DMF–ethanol for **1** and DMF–methanol for **2**) through the facile assembly reaction of an equimolar Ca^{II}–H_2BDC-F_4 mixture under ambient conditions (see Scheme 1). In **1**, ethanol and DMF are not included in the final crystalline product, and water serves as both the terminal ligand and the guest molecule. Notably, guest water molecules are involved in the intermolecular O–H···F hydrogen interactions with the fluorinated host framework responsible for the spontaneous formation of a chiral water network. As for **2**, when the solvent system was replaced with a mixture solvent of methanol and DMF, only the coordinated methanol occupies the potential channel space. Moreover, the difference in solvent systems also contributes to the different coordination modes of carboxylate groups, that is,

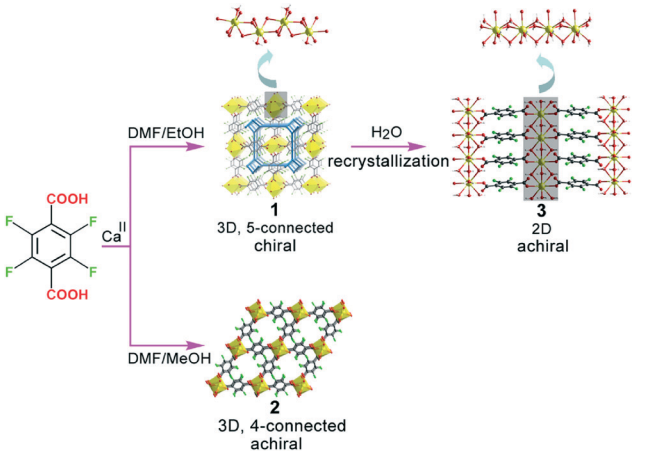

Scheme 1 Summary of the formation of chiral/achiral Ca-MOFs.

μ_2-η^1:η^1-bridging and μ_3-η^2:η^2-chelating/bridging for **1** (see Scheme 2a) and μ_2-η^1:η^1-*syn–anti*-bridging for **2** (see Scheme 2b). As a result, the different net topologies from binodal 5-connected for **1** to bimodal 4-connected for **2** are observed. The only difference in the synthetic process of **1** and **2** is the crystallization medium, illustrating the tuning effect of the solvent on the formation of such chiral or achiral Ca^{II} MOFs based on the achiral ligand $H_2BDC\text{-}F_4$.

Interestingly, both **1** and **2** exhibit water solubility and are insoluble in common organic solvents (such as alcohol, chloroform, acetonitrile and DMF). However, **1** is more highly water-soluble, with a solubility of *ca.* 130 mg mL^{-1}, than **2**, with a water solubility of *ca.* 20 mg mL^{-1}. Further, the molecular conductivity of the water solution of **1** and **2** at room temperature was determined. The observed values of molecular conductivity for **1** and **2** are 16.27 and 3.52 mS m^2 mol^{-1}, respectively, indicating that **1** should dissociate into ionic metal species and confirming its unusually high solubility. Thus, recrystallization of **1** in aqueous solution may occur readily. Upon slowly evaporating the water solution of **1**, a new Ca^{II} MOF, **3**, was successfully achieved. In contrast to **1**, an even higher water solubility of *ca.* 180 mg mL^{-1} was observed for **3**, and its molecular conductivity reached 21.52 mS m^2 mol^{-1} at room temperature. On the other hand, it should be pointed out that the procedure of water-induced structural conversion from **1 to 3** is irreversible since complex **3** is almost insoluble in DMF and ethanol.

Further structural comparison between **1** and **3** shows the effect of such water-induced transformation on the final frameworks. In **1**, the seven-coordinated Ca^{II} ion is completed by five $BDC\text{-}F_4$ dianions and one aqua ligand, while the nine-coordinated Ca^{II} center in **3** is surrounded by two $BDC\text{-}F_4$ dianions and seven aqua ligands. In contrast, the $BDC\text{-}F_4$ ligand in **3** shows a monodentate coordination mode (see Scheme 2c) for each carboxylate group. As a consequence, this leads to the generation of 1D $[Ca(COO)_2(H_2O)]_n$ for **1** and $[Ca(COO)_2(H_2O)_4]_n$ for **3** (see Scheme 1). In addition, the $BDC\text{-}F_4$ ligand displays distinct connectivities in the complexes **1** and **3** presented here (see Schemes 1a for **1** and c for **3**). Based on the abovementioned results, different coordination frameworks (3D for **1** and 2D for **3**) were obtained. This result illustrates that the superhydrophilic racemic mixture of chiral crystalline solids of **1** can be converted to the achiral MOF **3** when a large amount of water is introduced. To the best of our knowledge, such a drastic structural transformation for MOFs from 3D chiral to 2D achiral crystals induced by water has not been reported so far.

Stability and gas sorption properties of 1

Thermogravimetric analyses (TGA) of **1–3** indicate that solvent molecules were lost in the temperature ranges 45–160 °C (found: 10.61%, calculated: 11.52% for **1**), 20–130 °C (found: 19.46%, calculated: 18.81% for **2**) and 40–160 °C (found: 19.73%, calculated: 20.67% for **3**) (see Fig. S1†). Powder X-ray diffraction (PXRD) measurements of **1–3** show that the experimental PXRD patterns match well with the corresponding simulated ones obtained from single-crystal diffraction data (see Fig. S2 and S3†). To check the porosity of the fluorinated MOF **1**, a fresh sample was soaked with dry acetone and then activated under high vacuum at 160 °C for 6 h to generate the dehydrated framework **1a**. The PXRD pattern of **1a** matches that of the as-synthesized **1** (Fig. S2, ESI†), indicating that the anhydrous porous framework is maintained after removal of water from 1D channels. Gas adsorption of N_2 and CO_2 at 77 and 195 K, respectively, was further explored on the anhydrous porous framework **1a**. Adsorption analysis of N_2 shows negligible uptake while a surprisingly significant uptake is observed for CO_2 (81.1 cm^3 g^{-1} at 195 K) (see Fig. 5). The CO_2 sorption isotherm displays obvious hysteresis arising from the interactions between CO_2 molecules and the host framework. Fitting the Langmuir equation to the CO_2 sorption isotherm gives an estimated surface area of 348 m^2 g^{-1}. The selective sorption of CO_2 over N_2 can be primarily attributed to their different electrostatic interactions with the porous surface. For **1a**, besides the numerous F atoms in the channels being more attractive to CO_2 than other gases for strong quadrupole–quadrupole interactions,[30] the exposed Ca^{II} ions, stemming from the release of coordinated water molecules, can also result in an electric field interacting with a quadrupole

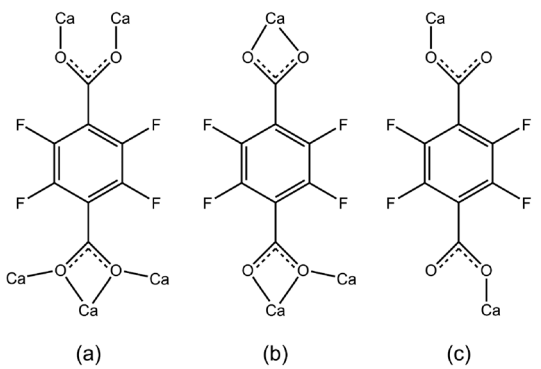

Scheme 2 Coordination modes of $BDC\text{-}F_4$ in **1–3**.

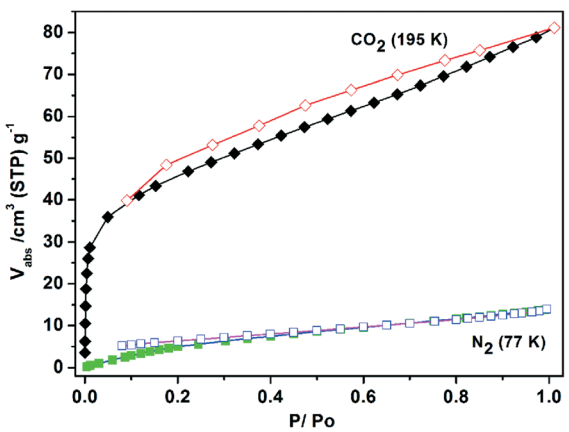

Fig. 5 Gas sorption isotherms of **1a** for N_2 (77 K) and CO_2 (195 K).

molecule such as CO_2. In addition, the smaller kinetic diameter of CO_2 (*ca.* 3.3 Å) than that of N_2 (3.64 Å) also enables more adsorbing sites to be accessed in the channels, thus filling the channels easily.

Conclusions

In summary, the construction of 3D chiral and achiral Ca-based MOFs can be realized based on a rigid achiral perfluorinated benzenedicarboxylate in different solvents. The chiral MOF framework hosts an unprecedented 3D chiral water network comprising two distinct helical water units; this perfluorous MOF also exhibits sorption selectivity to CO_2 and thus may have potential applications in the separation of greenhouse gases. Further, the superhydrophilic chiral MOF can act as a precursor to produce a new achiral 2D MOF by recrystallization in water along with a transformation from chiral to achiral crystals. More efforts on the halogen-induced effect on coordination assemblies of chiral MOFs with achiral halogenated ligands are currently under way.

Acknowledgements

This work was supported by the National Natural Science Foundation of China (21031002, 21101017, 21201026 and 21276029), the Jiangsu Key Laboratory of Advanced Catalytic Materials and Technology (BM2012110), the Nature Science Foundation of Jiangsu Province (BK20131142), the Open Foundation of Jiangsu Province Key Laboratory of Fine Petrochemical Technology (KF1105), and the Program for Innovation Team Building at the Institutions of Higher Education in Chongqing (KJTD201309).

Notes and references

1 (*a*) J. R. Li, J. Sculley and H. C. Zhou, *Chem. Rev.*, 2012, **112**, 869; (*b*) M. O'Keeffe and O. M. Yaghi, *Chem. Rev.*, 2012, **112**, 675; (*c*) C. Wang, T. Zhang and W. B. Lin, *Chem. Rev.*, 2012, **112**, 1084; (*d*) W. Zhang and R. G. Xiong, *Chem. Rev.*, 2012, **112**, 1163; (*e*) Y. J. Cui, Y. F. Yue, G. D. Qian and B. L. Chen, *Chem. Rev.*, 2012, **112**, 1126.

2 (*a*) T. Uemura, N. Yanai and S. Kitagawa, *Chem. Soc. Rev.*, 2009, **38**, 1228; (*b*) Z. Wang and S. M. Cohen, *Chem. Soc. Rev.*, 2009, **38**, 1315; (*c*) J. Lee, O. K. Farha, J. Roberts, K. A. Scheidt, S. T. Nguyen and J. T. Hupp, *Chem. Soc. Rev.*, 2009, **38**, 1450.

3 (*a*) D. Bradshaw, J. B. Claridge, E. J. Cussen, T. J. Prior and M. J. Rosseinsky, *Acc. Chem. Res.*, 2005, **38**, 273; (*b*) B. Kesanli and W. B. Lin, *Coord. Chem. Rev.*, 2003, **246**, 305.

4 S. C. Sahoo, T. Kundu and R. Banerjee, *J. Am. Chem. Soc.*, 2011, **133**, 17950.

5 (*a*) L. J. Barbour, G. W. Orr and J. L. Atwood, *Nature*, 1998, **393**, 671; (*b*) M. Zuhayra, W. U. Kampen, E. Henze, Z. Soti, L. Zsolnai, G. Huttner and F. Oberdorfer, *J. Am. Chem. Soc.*, 2006, **128**, 424; (*c*) B. Q. Ma, H. L. Sun and S. Gao, *Chem. Commun.*, 2005, 2336.

6 (*a*) S. Pal, N. B. Sankaran and A. Samanta, *Angew. Chem., Int. Ed.*, 2003, **42**, 1741; (*b*) M. H. Mir, L. Wang, M. W. Wong and J. J. Vittal, *Chem. Commun.*, 2009, 2336.

7 (*a*) B. Q. Ma, H. L. Sun and S. Gao, *Angew. Chem., Int. Ed.*, 2004, **43**, 1374; (*b*) Q. G. Meng, S. T. Yan, G. Q. Kong, X. L. Yang and C. D. Wu, *CrystEngComm*, 2010, **12**, 688.

8 (*a*) R. Carballo, B. Covelo, C. Lodeiro and E. M. Vázquez-López, *CrystEngComm*, 2005, **7**, 294; (*b*) Y. G. Huang, Y. Q. Gong, F. L. Jiang, D. Q. Yuan, M. Y. Wu, Q. Gao, W. Wei and M. C. Hong, *Cryst. Growth Des.*, 2007, **7**, 1385.

9 B. L. Wu, S. Wang, R. Y. Wang, J. X. Xu, D. Q. Yuan and H. W. Hou, *Cryst. Growth Des.*, 2013, **13**, 518.

10 K. Bhattacharyya, *Chem. Commun.*, 2008, 2848.

11 (*a*) B. Sreenivasulu and J. J. Vittal, *Angew. Chem., Int. Ed.*, 2004, **43**, 5769; (*b*) B. Zhao, P. Cheng, X. Y. Chen, C. Cheng, W. Shi, D. Z. Liao, S. P. Yan and Z. H. Jiang, *J. Am. Chem. Soc.*, 2004, **126**, 3012.

12 B. K. Saha and A. Nangia, *Chem. Commun.*, 2005, 3024.

13 (*a*) S. C. Chen, Z. H. Zhang, Q. Chen, L. Q. Wang, J. Xu, M. Y. He, M. Du, X. P. Yang and R. A. Jones, *Chem. Commun.*, 2013, **49**, 1270; (*b*) Z. H. Zhang, S. C. Chen, M. Y. He, C. Li, Q. Chen and M. Du, *Cryst. Growth Des.*, 2011, **11**, 5171.

14 (*a*) A. L. Spek, *J. Appl. Crystallogr.*, 2003, **36**, 7; (*b*) A. L. Spek, *PLATON, A Multipurpose Crystallographic Tool*, Utrecht University, Utrecht, The Netherlands, 2002.

15 Bruker AXS, *SAINT Software Reference Manual*, Madison, WI, 1998.

16 G. M. Sheldrick, *SHELXTL NT Version 5.1. Program for Solution and Refinement of Crystal Structures*, University of Göttingen, Germany, 1997.

17 H. D. Flack, *Acta Crystallogr., Sect. A: Found. Crystallogr.*, 1983, **39**, 876.

18 M. O'Keeffe, M. A. Peskov, S. J. Ramsden and O. M. Yaghi, *Acc. Chem. Res.*, 2008, **41**, 1782, and the Reticular Chemistry Structure Resource website at http://rcsr.anu.edu.au.

19 V. A. Blatov, A. P. Shevchenko and V. N. Serezhkin, *J. Appl. Crystallogr.*, 2000, **33**, 1193, see also http://www.topos.ssu.samara.ru.

20 C. Yang, X. Wang and M. A. Omary, *J. Am. Chem. Soc.*, 2007, **129**, 15454.

21 L. Infantes, J. Chisholm and S. Motherwell, *CrystEngComm*, 2003, **5**, 480.

22 The value is taken from the data at 200 K. D. Eisenberg and W. Kauzmann, *The Structure and Properties of Water*, Oxford University Press, Oxford, 1969.

23 (*a*) X.-Y. Duan, X. Cheng, J.-G. Lin, S.-Q. Zang, Y.-Z. Li, C.-J. Zhu and Q.-J. Meng, *CrystEngComm*, 2008, **10**, 706; (*b*) K.-L. Zhang, C.-T. Hou, J.-J. Song, Y. Deng, L. Li, S. W. Ng and G.-W. Diao, *CrystEngComm*, 2012, **14**, 590.

24 (*a*) E. Elacqua, P. Kaushik, R. H. Groeneman, J. C. Sumrak, D.-K. Bučar and L. R. MacGillivray, *Angew. Chem., Int. Ed.*, 2012, **51**, 1037; (*b*) T. L. Kinnibrugh, N. Garcia and A. Clearfield, *J. Solid State Chem.*, 2012, **187**, 149; (*c*) T. E. Clark, A. Martin, M. Makha, A. N. Sobolev, D. Su,

H. W. Rohrs, M. L. Gross and C. L. Raston, *Cryst. Growth Des.*, 2010, **10**, 3211.

25 S. G. Baca, H. Adams, C. S. Grange, A. P. Smith, I. Sazanovich and M. D. Ward, *Inorg. Chem.*, 2007, **46**, 9779.

26 B. F. Abrahams, C. T. Abrahams, M. G. Haywood, T. A. Hudson, B. Moubaraki, K. S. Murray and R. Robson, *Dalton Trans.*, 2012, **41**, 4091.

27 J.-B. Arlin, A. J. Florence, A. Johnston, A. R. Kennedy, G. J. Miller, K. Patterson, B. F. Abrahams, C. T. Abrahams, M. G. Haywood, T. A. Hudson, B. Moubaraki, K. S. Murray and R. Robson, *Cryst. Growth Des.*, 2011, **11**, 1318.

28 (*a*) C. P. Li and M. Du, *Chem. Commun.*, 2011, **47**, 5958; (*b*) X. Chen, S. B. Qiao, D. Liu, J. P. Lang, Y. Zhang, C. Xu and S. L. Ma, *CrystEngComm*, 2010, **12**, 1610; (*c*) Y. Chen, H. X. Li, D. Liu, L. L. Liu, N. Y. Li, H. Y. Ye, Y. Zhang and J. P. Lang, *Cryst. Growth Des.*, 2008, **8**, 3810.

29 (*a*) X. D. Chen, M. Du and T. C. W. Mak, *Chem. Commun.*, 2005, 4417; (*b*) T. Ezuhara, K. Endo and Y. Aoyama, *J. Am. Chem. Soc.*, 1999, **121**, 3279.

30 P. Pachfule, Y. Chen, J. Jiang and R. Banerjee, *Chem. – Eur. J.*, 2012, **18**, 688.

